

Sol-gel processing of transparent $\text{Lu}_2\text{O}_3:\text{Eu}^{3+}$ phosphor films

*N.V.Babayevskaya, A.S.Bezkrovnyi, P.V.Mateychenko,
O.M.Vovk, R.P.Yavetskiy*

Institute for Single Crystals, STS "Institute for Single Crystals", National Academy of Sciences of Ukraine, 60 Lenin Ave., 61001 Kharkiv, Ukraine

Received November 12, 2010

Sol-gel method has been used to fabricate homogeneous, transparent $\text{Lu}_2\text{O}_3:\text{Eu}^{3+}$ ($\text{Eu}^{3+} = 5$ at. %) films with thickness in the 100–300 nm range on sapphire substrates. The film morphology and structure has been studied by atomic force microscopy, scanning and transmission electron microscopy. The formation conditions of monolayer homogeneous films with average crystallite size of 20 nm have been determined. The luminescent properties of $\text{Lu}_2\text{O}_3:\text{Eu}^{3+}$ films depending on annealing temperature have been studied.

Золь-гель методом на сапфировых подложках получены однородные, прозрачные пленки $\text{Lu}_2\text{O}_3:\text{Eu}^{3+}$ ($\text{Eu}^{3+} = 5$ ат. %) с толщиной в диапазоне 100–300 нм. Морфология и структура пленок были исследованы с помощью атомно-силового микроскопа, сканирующей и просвечивающей электронной микроскопии. Определены условия формирования однослойных, гомогенных пленок со средним размером кристаллитов 20 нм. Изучены люминесцентные свойства пленок $\text{Lu}_2\text{O}_3:\text{Eu}^{3+}$ в зависимости от температуры отжига.

1. Introduction

Nowadays oxide scintillation materials are considered as promising materials for digital medical imaging and radiography [1]. Traditionally, CsI:Tl , $\text{Bi}_4\text{Ge}_3\text{O}_{12}$, CdWO_4 in the single crystalline form are used to convert X-rays into visible light. However, mass fabrication of bulk materials requires high energy and material consumption during crystal growth and machining processes, and is very expensive. During last two decades optical ceramics was introduced as an alternative for single crystalline X-ray detectors [2]. The modern technology of transparent ceramics production represents a multistage process that demands utilization of special hot pressing equipment [3]. Production of large area ceramics of high optical quality is a significant challenge. Moreover, to improve contrast and spatial resolution transparent ceramics should be pixilated into arrays of pixels [3], and re-

sulting resolution of scintillation ceramics will be limited among other factors by the pixel size (typically tens of microns).

Scintillation powdered screens and thin scintillating films are another class of materials for detection of X-rays. For example, micron sized $\text{Gd}_2\text{O}_2\text{S:Tb}^{3+}$ (GOS:Tb^{3+}) powders are widely used for highly efficient X-ray screens for medical diagnostics [4, 5]. Europium doped lutetium oxide $\text{Lu}_2\text{O}_3:\text{Eu}^{3+}$ is a new oxide inorganic scintillator which was introduced as one of the most perspective material for X-ray detectors due to excellent scintillation properties, chemical stability as well as high light conversion efficiency (approximately 80 % of CsI:Tl) [3], high density (9.4 g/sm^3) and effective atomic number $Z_{eff} = 63$ [6, 7]. Sharp emission in the red region of the spectrum (with a maximum at ~611 nm) allows one to use $\text{Lu}_2\text{O}_3:\text{Eu}^{3+}$ screens in combination with a-Si:H and CCD arrays. $\text{Lu}_2\text{O}_3:\text{Eu}^{3+}$ scintillation films was prepared by different tech-

niques [8, 9]. Large area screens based on micron sized $\text{Lu}_2\text{O}_3:\text{Eu}^{3+}$ powders possess a light yield comparable with commercial GOS: Tb^{3+} screens, but somewhat lower spatial resolution [9]. Improved spatial resolution of scintillation screens can be achieved with submicron or nanosized powders. For example, nano-crystalline film phosphors can show not only enhanced resolution [10], but also higher detection efficiency compared to commercially available phosphors with larger particle size when they are exposed by soft X-rays [11], what is very important for X-ray microscopy and other applications that require submicron resolution.

To obtain thin films or coatings of high optical quality with submicron spatial resolution, the uniform thickness of phosphor across the surface of the film is necessary. The structure of the layer should also be smooth and free from pores and cracks [10, 12]. Sol-gel technology is one of the most promising approach to obtain homogeneous, transparent films with controlled thickness and homogeneous distribution of activator in the phosphor lattice [13, 14]. Moreover, this technology requires much lower synthesis temperatures compared to classical solid-phase method [15]. The aim of this study is to obtain and characterize $\text{Lu}_2\text{O}_3:\text{Eu}^{3+}$ monolayer films with submicron thickness by simple spin-coating technique.

2. Experimental

Lutetium nitrate, europium nitrate ($C(\text{Eu}^{3+}) = 5$ at. %) and citric acid were used as starting reagents in sol-gel process [7, 16]. Stoichiometric amounts of nitrates were dissolved in 2-methoxyethanol with addition of citric acid. Ratio of metal cations to the citric acid anions ($\text{Me}^{3+}/\text{Cit}^-$) was 1:2. After complete dissolution of the precursor, formaldehyde was added as a drying-control chemical additive (DCCA) (by 2 % of the total solution volume). To obtain $\text{Lu}_2\text{O}_3:\text{Eu}^{3+}$ monolayer films the sapphire substrate was coated by 0.3 ml of the prepared suspension using spin-coating method. The concentration of rare-earth ions in the solution was 0.5–2.9 mol/l. The substrate rotation speed was 2000 rpm. The precursors deposited on the sapphire substrate were annealed in air in the $T = 600$ – 1200°C temperature range for 2 hours in order to form crystalline films. We used sapphire as a substrate due to its unique properties (high temperature resistance, toughness, chemical resistance and high transparency in a wide spectrum range)

[17]. In addition, good matching of oxides lattices will minimize thermal stresses during film formation.

The morphology of films was analyzed by means of scanning electron microscopy (SEM) with a JSM-6390LV (JEOL, Japan) and transmission electron microscopy (TEM) using EM-125 (Selmi, Ukraine) operating at accelerating voltage of 100 kV. The films thicknesses were determined from the SEM data. Atomic force microscope (AFM) SolverPRO was used to examine the smoothness of the films. Excitation and luminescence spectra in the range 200–800 nm were determined using a combined fluorescence spectrometer FLS 920 with a time resolution.

3. Results and discussions

To obtain thin, homogeneous and transparent films, we used suspensions obtained by sol-gel technique. The $\text{Lu}_2\text{O}_3:\text{Eu}^{3+}$ films were formed on sapphire substrates by spin-coating technique. Sol-gel method provides a high degree of homogenization of the initial components due to the complete dissolution of precursors in the starting solution. Crack and pore formation during drying process is one of the most serious problems in sol-gel processing of thin film. The pore size and liquid vapor pressure can be controlled by adding DCCA to the mixed metal-alkoxide solution. Ethylene glycol ($\text{HOCH}_2\text{CH}_2\text{OH}$) and formaldehyde are often used as DCCA [18]. Furthermore, to obtain transparent uniform films the order of reagents adding into suspension is extremely important. Direct mixing of starting materials (nitrates, citric acid and DCCA) with the solvent results in the rapid formation of monolithic gel. An increase in the synthesis time leads to gel solidification. In this regard, DCCA (formaldehyde) was added directly into the sol after several hours of mixing of the main components. Figure 1 shows the effect of DCCA addition on the morphology of the surfaces of $\text{Lu}_2\text{O}_3:\text{Eu}^{3+}$ films. As can be seen, the films obtained without DCCA are porous (Fig. 1a), while the addition of DCCA promotes formation of a homogeneous crack-free and pore-free films (Fig. 1b).

Concentration of rare earth ions in solution which determine the solution viscosity is one of the main parameters affecting the uniformity of the film. High concentration of the rare earth ions in solution ($C = 2.9$ mol/l) leads to the formation of cracks (Fig. 2a). This is due to the presence of two

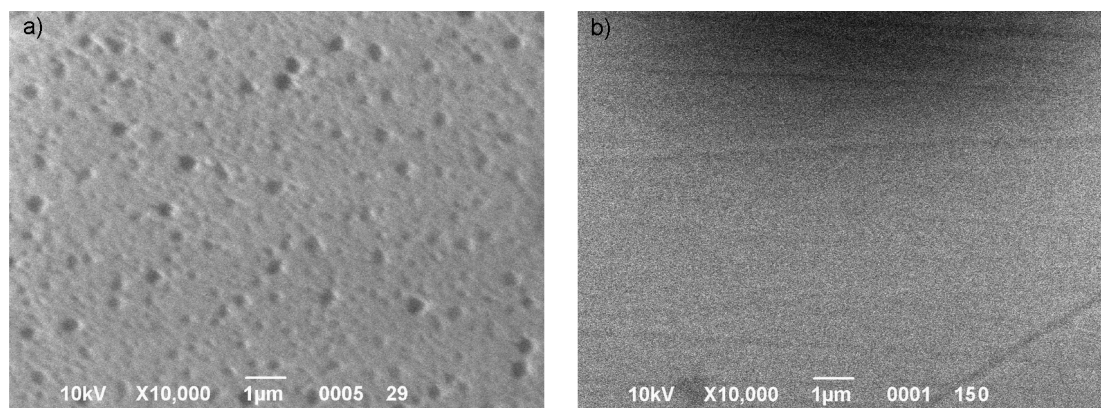


Fig. 1. SEM images of $\text{Lu}_2\text{O}_3:\text{Eu}^{3+}$ sol-gel film prepared without DCCA (a) and with DCCA (b) and annealed at $T = 800^\circ\text{C}$ for 2 h.

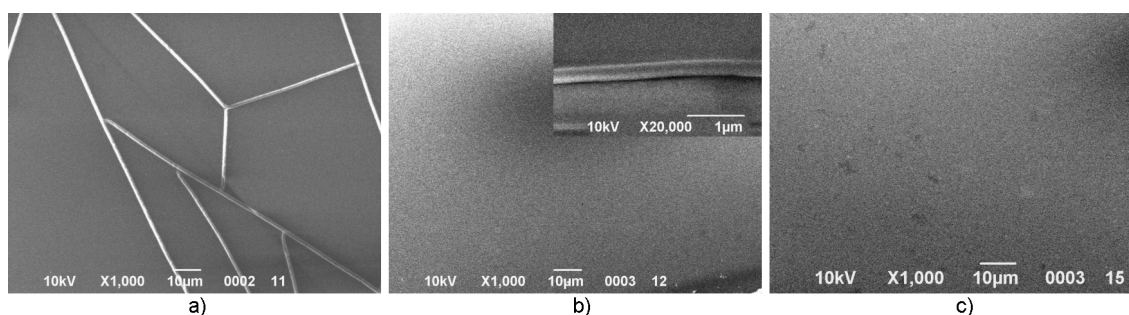


Fig. 2. SEM images of $\text{Lu}_2\text{O}_3:\text{Eu}^{3+}$ sol-gel films obtained from solution containing different concentrations of rare earth ions: $C = 2.9$ mol/l (a); $C = 1.4$ mol/l (b) and $C = 0.5$ mol/l (c). The inset in Fig. 2b shows the cross section of $\text{Lu}_2\text{O}_3:\text{Eu}^{3+}$ film.

liquids of different nature in the reaction system. These liquids increase the surface tension of the solvent (2-methoxyethanol) and, consequently, increase the capillary forces during drying. Decrease the rare earth ions concentration up to $C = 1.4$ mol/l and more (accompanying by subsequent solution viscosity decrease) leads to formation of a homogeneous films (Fig. 2b). Utilization of less concentrated solutions leads to the formation of thinner films in which some pores of 1–3 μm are presented after annealing. The pores formation can be caused by surface heterogeneity of the substrate due to faulty polishing of substrate or non-uniform drying of the film during deposition. However, it should be noted that deposition of the same amount of solution with different rare earth ions concentrations affects the thickness of resulting films. The film thickness was determined by scanning electron microscopy. The thickness of the monolayer $\text{Lu}_2\text{O}_3:\text{Eu}^{3+}$ sol-gel film depends on concentration of rare earth ions in solution and has a value in the 100–300 nm range (Fig. 2b, inset).

Fig. 3a show appearance of $\text{Lu}_2\text{O}_3:\text{Eu}^{3+}$ sol-gel film. The film was transparent; the measured in-line absorption coefficient was higher than 75 % in the visible wavelength range. The high transparency is very favorable for achieving high luminescence yield and homogenous distribution of the luminescence over the film surface. The AFM image of $\text{Lu}_2\text{O}_3:\text{Eu}^{3+}$ sol-gel film (Fig. 3b) demonstrates practically ideal smooth film topology for the sample annealed at 800°C . This allows one to consider sol-gel films as promising materials for modern X-rays digital imaging and radiography with submicron resolution.

The microstructure of $\text{Lu}_2\text{O}_3:\text{Eu}^{3+}$ sol-gel film was studied by TEM. Fig. 4 shows the fragment of $\text{Lu}_2\text{O}_3:\text{Eu}^{3+}$ film scraped away from the sapphire substrate. The film consists of near monodispersed close-packed nanocrystallites with average size of 10–20 nm. We have not measured the film density, however typical relatively densities for sol-gel film lie within 90–95 % range from the theoretical value [19, 20]. Some residual pores of 5 nm in diameter were observed

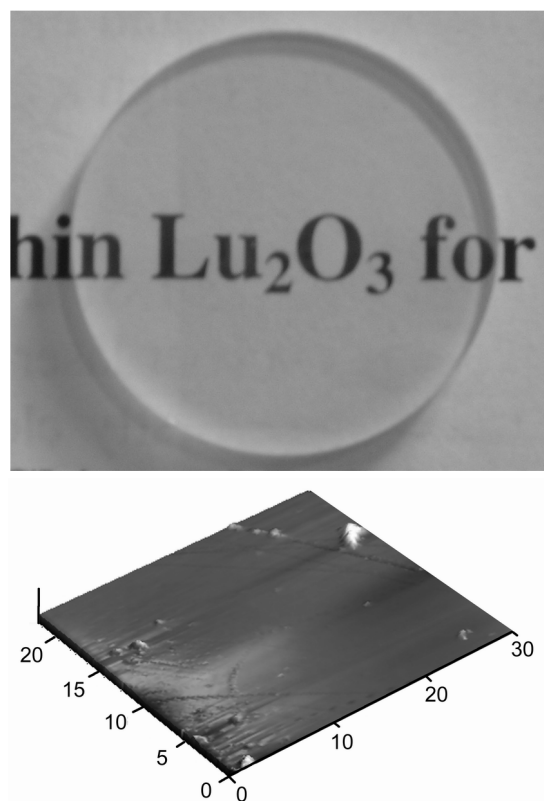


Fig. 3. As-prepared monolayer $\text{Lu}_2\text{O}_3:\text{Eu}^{3+}$ sol-gel film annealed at $T = 800^\circ\text{C}$ for 2 h (a) and AFM image of the film surface (b).

between the nanocrystallites. Extremely small size of residual pores (much smaller than the visible light wavelength) is one of the main factors governing the optical transparency of the obtained films. For example, some nanostructured ceramics with pore size smaller than 10 nm also possess

optical transparency [21, 22]. The selected area diffraction pattern in Fig. 4b verifies the polycrystalline structure of $\text{Lu}_2\text{O}_3:\text{Eu}^{3+}$ sol-gel film.

The photoluminescence spectrum of single-layer $\text{Lu}_2\text{O}_3:\text{Eu}^{3+}$ (5 at. %) sol-gel film consists of group of lines corresponding to $^5D_0 \rightarrow ^7F_J$ ($J = 0-4$) transitions in Eu^{3+} ions. This confirms that activator ions enter into crystal lattice of lutetium oxide in the trivalent state (Fig. 5). The luminescence maximum observed at $\lambda = 611$ nm corresponds to $^5D_0 \rightarrow ^7F_2$ electric dipole transitions in europium ions. The photoluminescence excitation spectrum for the emission line at $\lambda = 611$ nm is presented by a wide band with a maximum at 213.5 nm and less intense and less pronounced band in the 225–265 nm wavelength range. The excitation band placed at 213.5 nm corresponds to band-to-band excitation of impurity luminescence, because the fundamental absorption of Lu_2O_3 starts at 5.5 eV (226 nm) [23]. The excitation band at 225–265 nm wavelength range is $\text{Eu}^{3+}-\text{O}^{2-}$ charge transfer band. The high excitation efficiency of impurity luminescence of $\text{Lu}_2\text{O}_3:\text{Eu}^{3+}$ films is a consequence of efficient energy transfer processes from lattice to luminescence centers (europium ions) via hole recombination mechanism [24]. $\text{Lu}_2\text{O}_3:\text{Eu}^{3+}$ in the nanocrystalline form is known as a material that possesses multiplication of electronic excitations. The photonic multiplication starts at the energies of 2–4 E_g due to generation of secondary electron-hole pairs by hot carriers. This leads to increase of luminescence yield of Eu^{3+} -centers [24]. The multiplica-

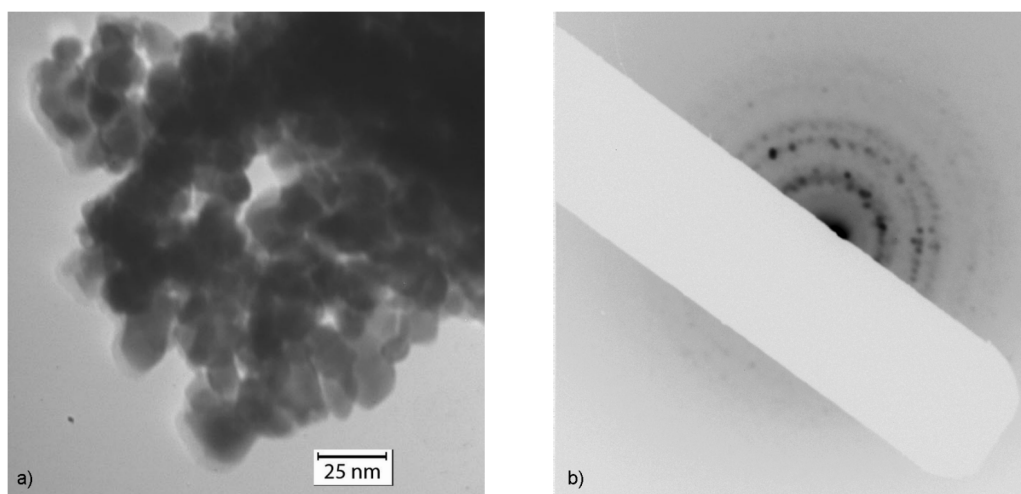


Fig. 4. The microstructure (a) and SAED pattern (b) of $\text{Lu}_2\text{O}_3:\text{Eu}^{3+}$ film annealed at $T = 800^\circ\text{C}$.

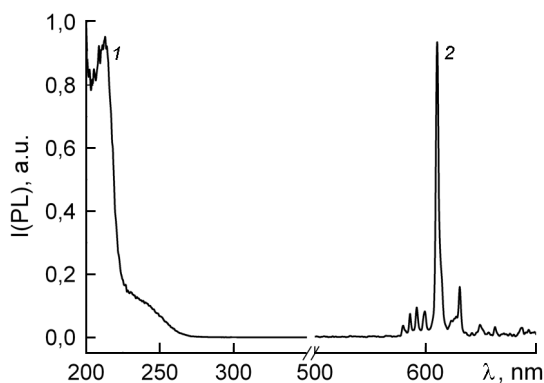


Fig. 5. Normalized room-temperature excitation (1) and luminescence (2) spectra of monolayer $\text{Lu}_2\text{O}_3:\text{Eu}^{3+}$ sol-gel film annealed at $T = 800^\circ\text{C}$ for 2 hours.

tion of electronic excitation in $\text{Lu}_2\text{O}_3:\text{Eu}^{3+}$ nanocrystals in the $h\nu > 14$ eV energy range is one of the reasons for their use as effective scintillators or phosphors with quantum yields higher than 1.

The luminescence spectrum of europium ions in $\text{Lu}_2\text{O}_3:\text{Eu}^{3+}$ sol-gel films is almost the same as for the bulk material [25]. However, the luminescence yield strongly depends on the size of crystallites, especially under high energy excitation. This is due to significant contribution of surface states to the relaxation of high energy excitation in nanocrystalline phosphors and films. The perturbed surface states are responsible for creation of a "dead" surface layer which leads to non-radiative losses on the surface defects and to a decrease in luminescence quantum efficiency [26]. Fig. 6 shows normalized photoluminescence yield of $\text{Lu}_2\text{O}_3:\text{Eu}^{3+}$ sol-gel films vs. annealing temperature. The temperature increase is accompanied by photoluminescence intensity rise which is probably connected with increase of average size of nanocrystallites. However, reaching the temperature of 1200°C leads to degradation of photoluminescence yield.

This fact is probably connected with intensification of diffuse mass transport processes, resulting in formation of non-uniform by the composition $(\text{Lu}_{1-x}\text{Eu}_x)_2\text{O}_3$ phase with Eu^{3+} ions concentration gradient inside the individual nanocrystallite, as it was recently shown for $\text{SiO}_2/(\text{Lu}_{1-x}\text{Eu}_x)_2\text{O}_3$ core-shell heterostructures [25]. As a result, luminescence of europium ions which have migrated to the crystallite surface will be

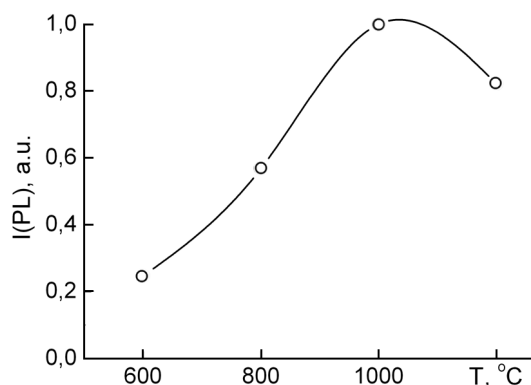


Fig. 6. Emission intensity of $\text{Lu}_2\text{O}_3:\text{Eu}^{3+}$ sol-gel films as a function of annealing temperature.

quenched, thus leading to decrease of photoluminescence intensity of films annealed at 1200°C . The degradation of luminescence yield with annealing temperature was recently observed for $\text{Y}_2\text{O}_3:\text{Eu}^{3+}$ films [27]. It should be noted that photoluminescence spectra of $\text{Lu}_2\text{O}_3:\text{Eu}^{3+}$ sol-gel films remain the same even for the annealing temperature of 1200°C indicating no solid-phase interaction on the "sapphire substrate — $(\text{Lu}_{1-x}\text{Eu}_x)_2\text{O}_3$ nanocrystalline film" interface.

4. Conclusions

Homogeneous single-layer $\text{Lu}_2\text{O}_3:\text{Eu}^{3+}$ (5 at. %) films with submicron thickness have been obtained by sol-gel process. The physico-chemical conditions for obtaining a crack-free film by sol-gel processing has been determined (concentration of rare earth ions in the 0.5–1.4 mol/l range, addition of DCCA). The film annealed at $T = 800^\circ\text{C}$ consist of near monodisperse close-packed nanocrystallites with diameter of 10–20 nm. The obtained $\text{Lu}_2\text{O}_3:\text{Eu}^{3+}$ films are transparent and demonstrate ideal smooth surface. The dependence of luminescence intensity of $\text{Lu}_2\text{O}_3:\text{Eu}^{3+}$ film on annealing temperature has been studied. The obtained results indicate that transparent nanocrystalline $\text{Lu}_2\text{O}_3:\text{Eu}^{3+}$ sol-gel films are promising materials for high-resolution detectors of X-rays.

The photoluminescence measurements by S.A.Vasyukov are greatly acknowledged. Some of the authors (R.P.Yavetskiy and N.V.Babayevskaya) are grateful for financial assistance of NAS of Ukraine through the grant for young scientists under contract No. A/8-09 from July 01, 2009.

References

1. M.Nikl, *Meas. Sci. Technol.*, **17**, 37 (2006).
2. C.Greskovich, S.Duclos, *Annu. Rev. Mater. Sci.*, **27**, 69 (1997).
3. A.Lempicki, C.Brecher, P.Szupryczynski et al., *NIM A*, **488**, 579 (2002).
4. S.Chatterjee, V.Shanker, H.Chander, *Mater. Chem. and Phys.*, **80**, 719 (2003).
5. E.-J.Popovici, L.Muresan, A.Hristea-Simoc et al., *Opt. Mater.*, **27**, 559 (2004).
6. E.Zych, D.Hreniak, W.Strek, *Mater. Sci.*, **20**, 111 (2002).
7. X.-J.Liu, H.-L.Li, R.-J.Xie et al., *J. Lumin.*, **127**, 469 (2007).
8. S.G.Topping, V.K.Sarin., *Int. J. Refr. Met. & Hard Mat.*, **27**, 498 (2009).
9. V.V.Nagarkar, S.R.Miller, S.V.Tipnis et al., *NIM B*, **213**, 250 (2004).
10. S.Kim, J.Park, S.Kang et al., *NIM A*, **576**, 70 (2007).
11. G.Fern, T.Ireland, J.Silver et al., *NIM A*, **600**, 434 (2009).
12. M.Gu, L.Zhu, X.Liu et al., *J. Alloys and Comp.*, **501**, 371 (2010).
13. M.L.Pang, J.Lin, J.Fu et al., *Opt. Mat.*, **23**, 547 (2003).
14. A.Garcia-Murillo, C.Le Luyer, C.Pedrini, J.Mugnier, *J. Alloy. Comp.*, **74**, 323 (2001).
15. S.K.Ruan, J.G.Zhou, A.M.Zhong et al., *J. Alloy. Comp.*, **72**, 275 (1998).
16. H.Guo, M.Yin, N.Dong et al., *App. Surf. Sci.*, **243**, 245 (2005).
17. J.Y.Cho, K.Y.Ko, Y.R.Do, *Thin Sol. Films*, **515**, 3373 (2007).
18. G.Facchini, A.Zappettini, A.Canali et al., *Opt. Mater.*, **17**, 251 (2001).
19. Garcia-Murillo, C.L.Luyer-Urlacher, C.Dujardin et al., *J. Sol-gel Techn.*, **26**, 957 (2003).
20. A.J.Morales Ramirez, A.Garcia Murillo, F.J.Carrillo Romo et al., *Thin Sol. Films*, **517**, 6753 (2009).
21. S.R.Casolco, J.Xu, J.E.Garay, *Scrip. Mater.*, **58**, 516 (2008).
22. E.A.Vovk, T.G.Deineka, A.G.Doroshenko et al., *J. Sup. Mater.*, **31**, 252 (2009).
23. S.Kimura, F.Arai, M.Ikezawa, *J. Phys. Soc. Jap.*, **69**, 3451 (2000).
24. V.N.Makhov, Ch.Lushchik, A.Lushchik et al., *J. Lum.*, **129**, 1711 (2009).
25. Q.Chen, Y.Shi, L.An et al., *J. Am. Ceram. Soc.*, **89**, 2038 (2006).
26. H.S.Yang, K.S.Hong, S.P.Feofilov et al., *J. Lum.*, **83-84**, 139 (1999).
27. J.Y.Cho, K.Y.Ko, Y.R.Do, *Thin Sol. Films*, **515**, 3373 (2007).

Золь-гель метод отримання прозорих $\text{Lu}_2\text{O}_3:\text{Eu}^{3+}$ плівок

**Н.В.Бабаєвська, О.С.Безкровний, П.В.Матейченко,
О.М.Вовк, Р.П.Явецький**

Золь-гель методом на сапфірових підкладках отримано однорідні, прозорі плівки $\text{Lu}_2\text{O}_3:\text{Eu}^{3+}$ ($\text{Eu}^{3+} = 5$ ат. %) з товщиною в діапазоні 100–300 нм. Морфологію та структуру плівок було досліджено за допомогою атомносилового мікроскопа, скануючої та просвічуючої електронної мікроскопії. Визначено умови формування одношарових, гомогенних плівок з середнім розміром кристалітів 20 нм. Вивчено люмінесцентні властивості плівок $\text{Lu}_2\text{O}_3:\text{Eu}^{3+}$ в залежності від температури відпалу.